

## Seepage Estimation from Canals Using Neural Networks

Ahmed M. Tawfik

Assistant professor, Irrigation and Hydraulics Department, Faculty of Engineering, Cairo University, Cairo, Egypt  
[ahmedmohamedtawfik@yahoo.com](mailto:ahmedmohamedtawfik@yahoo.com)

**Abstract:** Conservation of water supplies became very important as the demand increases. Water loss due to seepage from open channels represents one of the major components of water loss. Seepage occurs from open channels to the adjacent land due to the difference in water head between the water levels in the channels and the water table at the adjacent land. The aim of this study is to verify Hydrus software package with analog solutions like Bouwer's approach and to use Hydrus to estimate seepage from canals for many cases that cannot be solved by Bouwer's approach. Synthetic realizations were generated using Hydrus. Artificial neural networks (ANNs) were trained and verified using previous realizations to estimate seepage from canals for two cases. The results showed that ANN can estimate the seepage from canals simply, easily, and in no time.

[Ahmed M. Tawfik. **Seepage Estimation from Canals Using Neural Networks**. *Life Sci J* 2019;16(3):19-26]. ISSN: 1097-8135 (Print) / ISSN: 2372-613X (Online). <http://www.lifesciencesite.com>. 3. doi:[10.7537/marslsj160319.03](https://doi.org/10.7537/marslsj160319.03).

**Keywords:** seepage; canals; simulation; Hydrus; neural networks

### 1. Introduction

Conservation of water supplies became very important as the demand increases and it is hard to find new water sources. Water loss due to seepage from open channels represents one of the major components of water loss. The rates of seepage can be obtained by either direct measurements or by estimation. Seepage occurs from open channels to the adjacent land due to the difference in water head between the water levels in the channels and the water table at the adjacent land.

Several analytical solutions for steady state seepage from open channels were developed by some researchers. For example, the seepage from open channels by curvilinear cross section in very deep soil with no water table is treated [1]. Moreover, solutions to the seepage from trapezoidal channels to drainage layers at finite and infinite depths were proposed [2]. A solution for the seepage problem from an open channel embedded in uniform soil with a shallow water table that merges with the channel water level was proposed [3]. Electric resistance network analogs in studying the seepage from open channels was used [4-5]. The approach of Bouwer covers a wide range of water depths in channels, channel shapes, soil conditions, and positions for the water table. He also presented readily applicable graphs.

Simple algebraic equations for seepage loss computation from trapezoidal, rectangular, and triangular canals have been proposed [6]. Using these equations and the uniform flow equation, equations to determine the design variables to achieve minimum seepage loss from channel sections have been obtained for each shape of the three channel sections by applying Lagrangian optimization technique.

The seepage analysis of lined and unlined irrigation channels has been done using equations derived by Swamee et al. [7]. Their results showed that lining of canals can reduce seepage from canals by nearly 95%.

Analytical solutions that estimate the seepage rate from canals are over simplified due to its several assumptions that are rarely met in the field. Hence, there is a need to create a tool that is capable of estimating seepage with practical conditions. Due to the increase in computer speed, and the availability of numerical models which simulate the distribution of water content in saturated and unsaturated soils, several researchers became interested in using these models. Hydrus (2d/3d) is a famous computer software package that is capable of simulating the movement of water in variably saturated porous media. The verification of this model in simulating soil water distribution and movement were done by many researchers. For example, Hydrus-2d was used to simulate water flow and distribution around a line source in the unsaturated zone [8]. The results were compared with observed field data taken from sandy loam soil. An excellent agreement between the observed and simulated soil moisture data was found.

Hydrus-2d was used to simulate the distribution of soil water content around porous clay pipe in the vadose zone [9]. A good agreement was observed between the simulated and measured water contents. More over, a correlation coefficient of 0.98 was observed between the measured and simulated water contents.

Hydrus (2d/3d) is a software package which simulates the flow of water in a variably saturated porous media by solving Richard's equation

numerically using a Galerkin finite element method. This equation is shown below.

$$\frac{\partial \theta}{\partial t} = \nabla \cdot [K \nabla (h + z)] \quad (1)$$

Where  $\theta$  is the volumetric soil water content ( $L^3 L^{-3}$ ),  $h$  (L) is the soil water matric head,  $z$  (L) is the depth, and  $K$  is the unsaturated hydraulic conductivity tensor ( $LT^{-1}$ ).

Richard's equation is nonlinear for unsaturated flow as the volumetric soil water content and hydraulic conductivity  $K$  are nonlinear functions of the dependent variable soil moisture pressure head. In order to solve this equation, explicit expressions between the dependent variable matric head and the nonlinear terms  $\theta$  and  $K$  are required. There are many soil moisture relationships reported in literature. The most popular ones are by Van [10] where the closed form relationship between  $\theta$  and  $h$  developed by fitting mathematical equations to measured experiments data yields the following equation [10].

$$\theta(h) = \begin{cases} \theta_s & h \geq 0 \\ \theta_r + \frac{[\theta_s - \theta_r]}{[1 + |\alpha h|]^n]^m} & h < 0 \end{cases} \quad (2)$$

where  $\theta$  is moisture content at soil matrix potential;  $\theta_r$  is residual water content;  $\theta_s$  is saturated water content;  $h$  is soil water matric head; and  $m$ ,  $n$ , and  $\alpha$  are curve fitting parameters. The statistical pore size distribution model of [11] was used by [10] along with Eq. (2) to yield the relationship between  $K$  and  $h$ .

$$K(h) = \begin{cases} K_s, & h \geq 0 \\ K_s S_e^l \times [1 - (1 - S_e^m)^m]^2, & h < 0 \end{cases} \quad (3)$$

where  $K_s$  is the saturated hydraulic conductivity of the soil,  $l$  is a pore-connectivity parameter, and  $S_e$  and  $m$  are calculated from the following explicit equations:

$$m = 1 - \frac{1}{n}, n > 1 \quad (4)$$

$$S_e = \frac{\theta - \theta_r}{\theta_s - \theta_r} \quad (5)$$

Artificial neural networks (ANNs) have been used in many applications related to groundwater. For example, ANNs were used to predict soil water retention and saturated and unsaturated hydraulic conductivity from textural classes [12].

The aim of this study is to create two neural networks that can predict seepage rate from canals for two cases. This can be done by verifying Hydrus (2d/3d) software package with analog solutions like Bouwer's approach and to use Hydrus to generate synthetic realizations to estimate the seepage from

canals for different canal water depth ( $y$ ), different height between canal water level and groundwater table at ten times the bed width ( $h_a$ ), different distance between the canal bed and the bottom impervious layer ( $D_a$ ), different canal side slopes ( $t$ ), and different soil types (Fig. 1). ANNs were trained and verified using the previous realizations to estimate seepage from canals for the first case. Another case of seepage from canals with different parameters was analyzed (Fig. 2). In the second case, there is a pervious layer at the bottom of the simulated domain and the ground water table is far and deep in this pervious layer. Hydrus was used to generate synthetic realizations to estimate the seepage from canals for different canal water depths ( $y$ ), different height between canal water level and the pervious layer ( $h_b$ ), and different canal side slopes ( $t$ ). ANNs were trained and verified using the previous realizations to estimate seepage from canals for the second case.

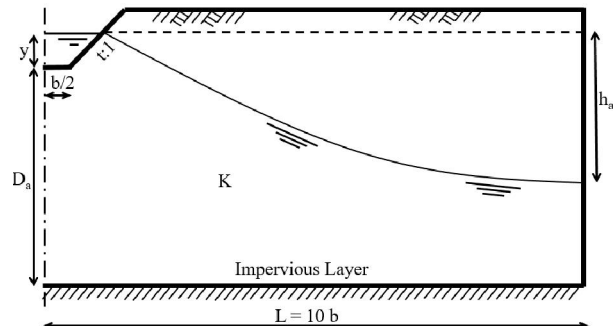


Fig. 1. Parameters for the first case.

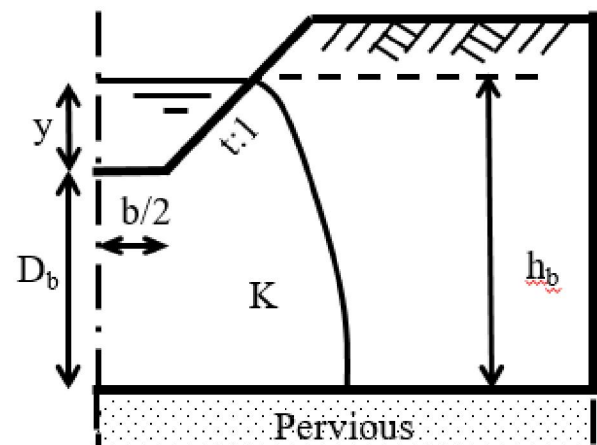


Fig. 2. Parameters for the second case.

McCulloch and Pitts developed the concept of ANNs in 1943. ANNs are models that simulate the structure and functioning of the human brain. An ANN is a massively parallel-distributed information-processing system that has certain performance characteristics resembling biological networks of the human brain (e.g., [13-14]). ANNs were developed

based on assumptions that information processing occurs at many neurons, signals pass between neurons through links, the signals transmitted are multiplied by associated weights of the links, and each neuron applies an activation function to determine its output signal [15]. ANNs were used in modelling many hydrologic processes such as rainfall-runoff, water quality simulation, stream flow, precipitation analysis, and groundwater management.

## 2. Materials And Methods

The simulated domain of a sample of realizations (first run in table 1) is 20 m width and 10 m depth as

shown in Fig. 3. The ground water level at ten times the bed width of the canal is below the soil surface by 6 m. Existing irrigation canal at the upper left corner of the simulated domain has 2 m bed width, 1 m water depth, 1:1 side slope, and 1 m free board. An impervious layer is located at a depth of 10 m at the bottom of the simulated domain. The flow domain was discretized with 8293 nodes and 16276 triangular elements. The dimensions of the finite elements grid were small enough to achieve high accuracy and avoid instability (Fig. 4). The finite element mesh was generated using the automatic triangulation algorithm that is implemented in HYDRUS [16].

**Table 1 Seepage rate from canal using Bouwer's solution and Hydrus software for different canal water depths, different height between canal water level and groundwater table at ten times the bed width, different distance between the canal bed and the bottom impervious layer, and different soil types.**

No.	y (m)	h (m)	D (m)	b (m)	Side slope	Soil type	K (m/d)	Bouwer's seepage rate (m <sup>3</sup> /d/m)	Hydrus Seepage rate (m <sup>3</sup> /d/m)
1	1	5	8	2	1:1	Loam	0.25	0.649	0.650
2	0.5	5	8	2	1:1	Loam	0.25	0.524	0.531
3	1.5	5	8	2	1:1	Loam	0.25	0.749	0.757
4	1	4	8	2	1:1	Loam	0.25	0.549	0.559
5	1	6	8	2	1:1	Loam	0.25	0.699	0.714
6	1	5	6	2	1:1	Loam	0.25	0.499	0.499
7	1	5	10	2	1:1	Loam	0.25	0.749	0.755
8	1	5	8	2	1:1	Sandy Loam	1.06	2.759	2.749
9	1	5	8	2	1:1	Clay Loam	0.06	0.162	0.163
10	1	5	8	2	1:1	Sandy clay	0.03	0.075	0.075

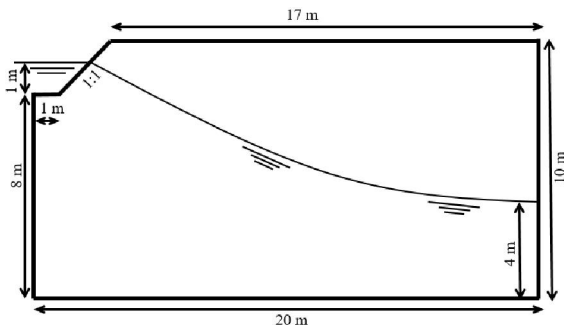


**Fig. 3. Geometry for the simulated domain (first case).**

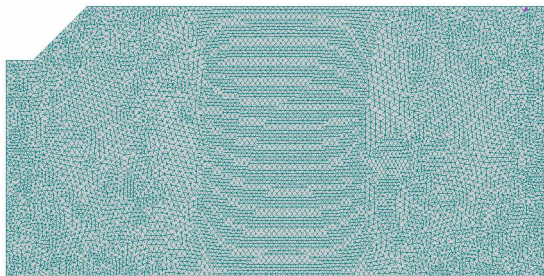


**Fig. 4. Finite element mesh of the simulated domain (first case).**

The boundary condition is assigned as no flux to all the edges of the simulated domain except the upper left corner and the bottom right side. The upper left corner around the channel, the boundary condition is constant head with time and variable head with depth. The pressure head changes linearly from zero at the water surface to  $y$  at the bottom of the channel. The bottom right side has a boundary condition of constant head with time and variable head with depth. The pressure head varies linearly from zero at the water surface to  $(D_a + y - h_a)$  at the bottom right corner (Fig. 5).

The soil is assumed as loam and its hydraulic parameters are taken from a soil catalog in Hydrus. The parameters of the loam soil from this catalog are  $\Theta_s = 0.43$ ,  $\Theta_r = 0.078$ ,  $\alpha = 3.6 \text{ m}^{-1}$ ,  $K_s = 0.2496 \text{ m d}^{-1}$ ,  $n = 1.56$  and  $l = 0.5$ . The parameters in this catalog were taken from [17] for the van Genuchten model. The initial soil profile is assumed as variable pressure head. The pressure varies linearly with depth. It has a value of 4 m at the bottom of the domain and -2 m at the soil surface as shown in Fig. 6. The final time is assigned as a large number (1000 days) in order to reach the steady state condition. The initial condition does not affect the soil water distribution at the steady

state but it should be assigned to Hydrus (2d/3d) to start computations.

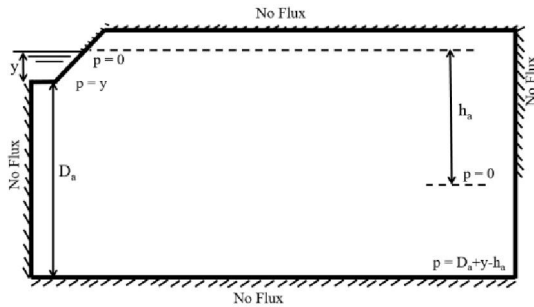


Fig. 5. Boundary conditions for each side of the simulated domain for the first case.

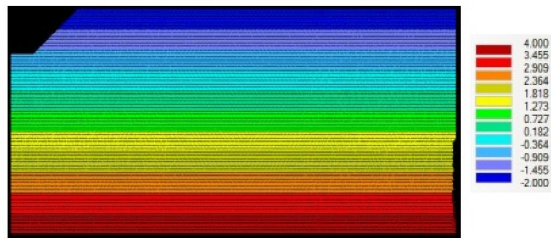


Fig. 6. Initial condition for the simulated domain.

In order to verify Hydrus (2d/3d), ten runs were performed using Hydrus (2d/3d) to estimate the seepage from the canal to the groundwater. The seepage results from Hydrus (2d/3d) is compared by the results of Bouwer analog solutions as shown in table 1. Moreover, Hydrus (2d/3d) is used to estimate seepage rate to the groundwater for one hundred realizations. The one hundred realizations are used to train and verify the ANN for the first case. The suitable number of realizations required to train and verify the network is determined by trial and error until the correlation coefficient between the output values from ANNs and the targets is close to one after testing the network. The network is trained to produce the ratio between the discharge and the multiplication of saturated hydraulic conductivity and the bed width  $Q/(K_s b)$  when it receives the ratio between the canal water depth and the canal bed width ( $y/b$ ), canal side slope ( $t$ ), the distance between the bed of the canal and the impervious layer divided by canal bed width ( $D_a/b$ ), the distance between the canal water level and the groundwater level at ten times the bed width divided by the canal bed width ( $h_a/b$ ) as shown in Fig. 7.

The design of the ANN is the determination of the number of hidden layers and the number of nodes in each hidden layer. This is achieved by trial and error. The input and output layers have pre-fixed numbers of nodes determined based on the training data groups. The input layer of the neural network has

four nodes that receive ( $y/b$ ), ( $t$ ), ( $D_a/b$ ), and ( $h_a/b$ ), while the output layer has one node corresponding to  $Q / (K_s b)$ . The best design for this network is two hidden layers. The first hidden layer has 5 nodes while the second hidden layer has 9 nodes. The two hidden layers have tan-sigmoid transfer, whereas the output node has a linear transfer function as shown in Fig.7.

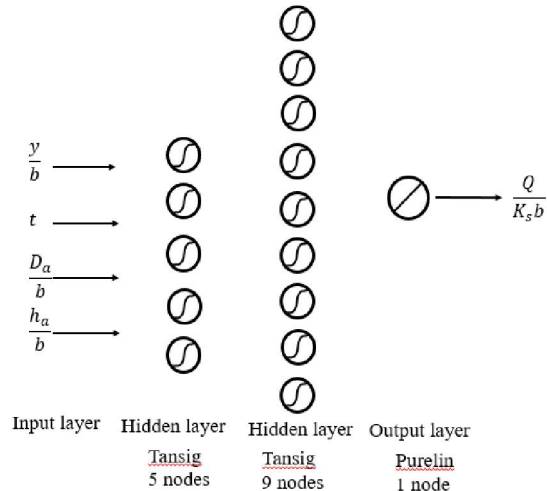


Fig. 7 Structure of the neural network. The hidden layers nodes have a tan-sigmoid transfer function and the output layer node has a linear transfer function.

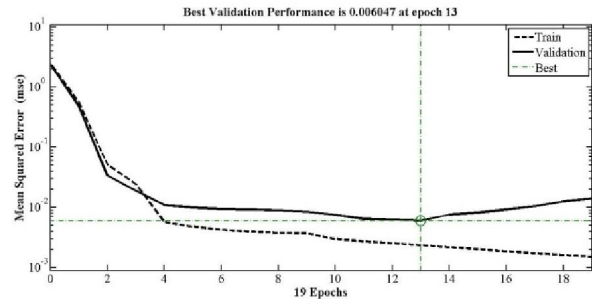
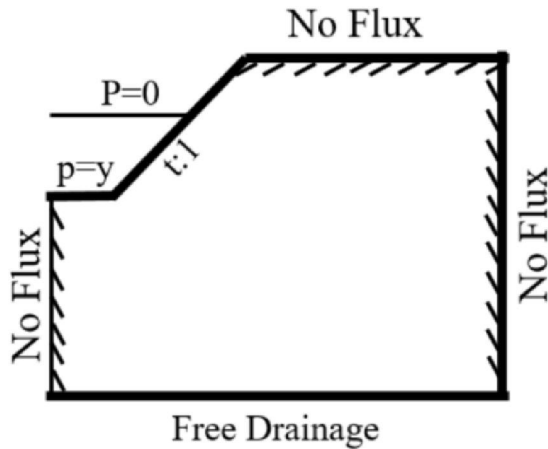


Fig. 8 A record of the ANN training and validation errors during the training process.

The input and output vectors generated according to Hydrus (2d/3d) are used to train the network. Before training process, the input and output vectors are normalized to a new group with unit standard deviation and zero mean. Then, the data is divided into two groups. The first group is the training group while the second is the validation group. The first group consists of two thirds of the data while the second group consists of the remaining third of the data. The first group is introduced to the ANNs to adjust its weights and extract the required input-output relation while the second group is used to prevent over fitting of the ANNs. This is achieved by stopping the training of the ANNs when the validation accuracy for the

second group deteriorates. This is an indication of over fitting for the relationship between the input and output (Fig.8). Although the validation group is used during the training of the ANNs, it does not affect the learning relationship between input and output. It is a control group to ensure better generalization and prevent over fitting of the trained ANNs when it used with other realizations.



**Fig. 9. Boundary conditions for each side of the simulated domain for the second case.**

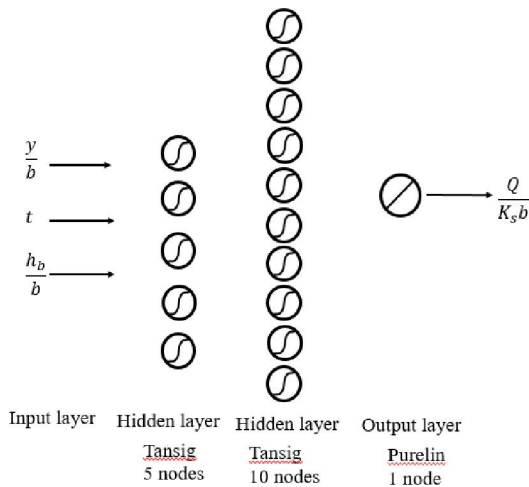


**Fig. 10 Structure of the second neural network. The hidden layers nodes have a tan-sigmoid transfer function and the output layer node has a linear transfer function.**

Sixty synthetic realizations was generated using Hydrus for the second case. The boundary conditions for this case is assigned as “No Flux” for all edges except the bottom edge and the upper left corner as shown in Fig. 9. The bottom edge is assigned as “Free Drainage” and the upper left corner is assigned as constant pressure head with time variable with space. The pressure head is 0 at the water surface while it is

equal the water depth at the bottom of the channel and it varies linearly between the two positions. Steady state simulation was performed by assigning the final time with a large number (1000 days) in the unsteady state. The previous realizations have different water depths, different side slopes, and different height between canal water level and the pervious layer. Another ANN was trained and validated for the second case to predict  $Q / (K_s b)$  when it receives  $(y/b)$ ,  $(t)$ , and  $(h_b/b)$  as shown in Fig.10. The input and output layers have pre-fixed numbers of nodes determined based on the training data groups. The input layer of the second neural network has three nodes that receive  $(y/b)$ ,  $(t)$ , and  $(h_b/b)$ , while the output layer has one node corresponding to  $Q / (K_s b)$ . The best design for this network is two hidden layers. The first hidden layer has 5 nodes while the second hidden layer has 10 nodes. The two hidden layers have tan-sigmoid transfer, whereas the output node has a linear transfer function as shown in Fig. 10.

The input and output vectors generated according to Hydrus (2d/3d) for the second case are used to train the network. Before training the network, the input and output vectors are normalized to a new group with unit standard deviation and zero mean. Then, the data is divided into two groups. The first group is the training group while the second is the validation group. The second network is trained until the validation accuracy for the second group deteriorates. This is an indication of over fitting for the relation between the input and output (Fig. 11).

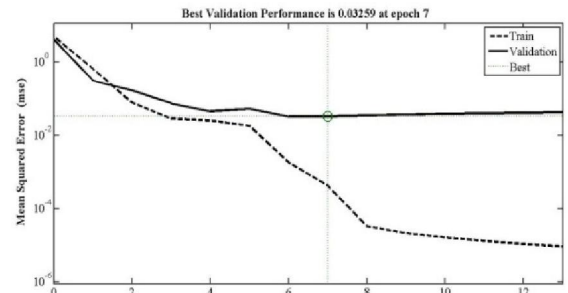


**Fig. 11 A record of the ANN training and validation errors during the training process.**

### 3. Results and Discussions

A comparison between the seepage rates from irrigation canal estimated using Bouwer’s analog solution and using a numerical model, Hydrus (2d/3d), is performed. Ten simulations were performed using Hydrus (2d/3d) and Bouwer’s analog solution for different canal water depths, different height between canal water level and groundwater table at ten times the bed width, different distance between the canal bed and the bottom impervious layer, and different soil types for the first case. The results from Hydrus

(2d/3d) and Bouwer’s solutions are plotted against each other, Fig. 12. The best line that fits the relation between Hydrus (2d/3d) and Bouwer’s solutions is also plotted with its equation and the correlation coefficient between the two solutions is also presented. The slope of the best line is 0.9951 which is very close to one and the y intercept is 0.0074 which is very close to zero. Moreover, the correlation coefficient between the two solutions is 0.9999 which is very close to one. This means that the results estimated using Hydrus (2d/3d) are very close to the estimated using Bouwer’s analog solution. This is an indication that Hydrus (2d/3d) is verified and can be used to estimate the seepage from canals with high accuracy.

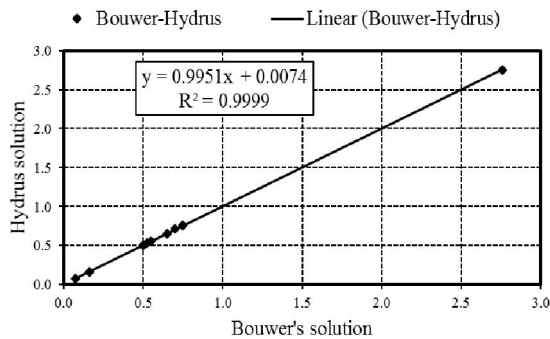


**Fig. 12. Relation between Bouwer solution and Hydrus solution. Moreover, the best line that fits the data is presented with its equation and correlation coefficient**

Bouwer’s analog solution is limited to canal side slope of 1:1, homogenous soil, and regular domain geometry. These conditions are rarely met in the field. Hence, there is a need to use a tool that is capable of estimating canal seepage rate without the previous constrains. Hydrus (2d/3d) can do this.

After training the first network, it should be tested. It should be able to predict output from input that has not been introduced to the network before. This step is known as generalization of the network. If the network has been properly trained, it should be able to generalize what it has learned to other cases not involved in training and validation. A group consisting of 10 input vectors obtained from 10 realizations is introduced to the first network. The seepage predicted by the first network is then compared to the actual values obtained by the traditional approach using Hydrus (2d/3d). Fig. 13 shows the comparison between the dimensionless seepage  $Q/(K_s b)$  obtained by ANN and those obtained by traditional method using Hydrus (2d/3d). The agreement is very high between the calculated values using Hydrus (2d/3d) and predicted values using ANN. Correlation  $R^2$  values between the calculated

and predicted values is 0.9535 which indicates a very good agreement. From the above results it is obvious that the network is able to generalize what it has learned to new realizations.

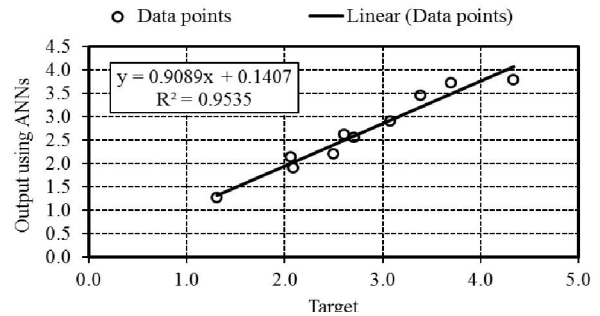


**Fig. 13. Comparison between  $Q/(K_s b)$  calculated using ANNs and the traditional method using Hydrus (2d/3d) for the first case.**

After training the second network for the second case, it should be tested. It should be able to predict output from input that has not been introduced to the network before. A group consisting of 15 input vectors obtained from 15 realizations is introduced to the second network. The seepage predicted by the second network is then compared to the actual values obtained by the traditional approach using Hydrus (2d/3d). Fig. 14 shows the comparison between the dimensionless seepage  $Q/(K_s b)$  obtained by ANN and those obtained by traditional method using Hydrus (2d/3d). The agreement is very high between the calculated values using Hydrus (2d/3d) and predicted values using ANN. Correlation  $R^2$  between the calculated and predicted values is 0.9916 which indicates a very good agreement. From the above results it is obvious that the second network is able to generalize what it has learned to new realizations for the second case.

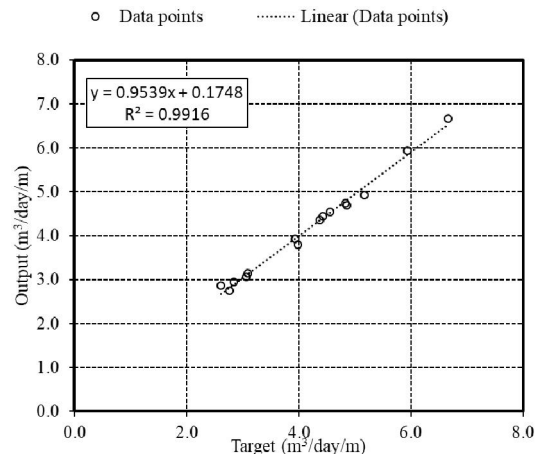


**Fig. 14. Comparison between  $Q/(K_s b)$  calculated using ANNs and the traditional method using Hydrus (2d/3d) for the second case.**

#### 4. Summary and Conclusions

Seepage occurs from open channels to the adjacent land due to the difference in water head between the water levels in the channels and the water table at the adjacent land. The aim of this study is to verify Hydrus (2d/3d) software package with analog solutions like Bouwer's approach and to use Hydrus to simulate soil water movement and distribution between canal water level and groundwater table to estimate the seepage from the canal for two cases. The simulations were performed at steady state by putting a large value to the final time in the unsteady state. Then, Hydrus (2d/3d) is used to make a large number of realizations. These realizations are introduced to the first ANNs to learn the relation between the input and target. By testing the first network, it is clear that the network is capable of estimating the dimensionless seepage  $Q / (K_s b)$  when it receives  $(y/b)$ ,  $(t)$ ,  $(D/b)$ , and  $(h/b)$  for the first case. Moreover, testing the second network ensures that it is capable of predicting  $Q / (K_s b)$  when it receives  $(y/b)$ ,  $(t)$ , and  $(h/b)$  for the second case. The correlation coefficients between the predicted values using ANNs and the calculated using Hydrus (2d/3d) are close to one which indicates a good prediction of the two networks. The comparison between the seepage rates from irrigation canal estimated using Bouwer's analog solution and using a numerical model, Hydrus (2d/3d) for the first case showed that Hydrus (2d/3d) is verified and can be used to estimate the seepage from canals with high accuracy. Hydrus (2d/3d) is more efficient than other analytical and/or analog solutions as it can be used even if the existing field conditions is complicated or the canal cross section is irregular. The approach of using ANNs to estimate seepage from canals is simple, easy, and takes no time.

#### List of symbols

$D_a$  (L) is the distance between the canal bed and the bottom impervious layer for the first case,  
 $D_b$  (L) is the distance between the canal bed and the bottom pervious layer for the second case,  
 $h$  (L) is the soil water matric head,  
 $h_a$  (L) is the height between canal water level and groundwater table at ten times the bed width for the first case,  
 $h_b$  (L) is the height between canal water level and the pervious layer for the second case,  
 $K$  ( $LT^{-1}$ ) is the unsaturated hydraulic conductivity tensor ( $LT^{-1}$ ),  
 $K_s$  ( $LT^{-1}$ ) is the saturated hydraulic conductivity of the soil,  
 $m$  is curve fitting parameter,  
 $n$  is curve fitting parameter,  
 $Q$  ( $L^3T^{-1}$ ) is the seepage discharge from the canal,  
 $t$  is the canal side slope,

$y$  (L) is the canal water depths  
 $z$  (L) is the depth,  
 $\alpha$  is curve fitting parameter,  
 $\Theta$  is the volumetric soil water content,  
 $\Theta_r$  is residual water content,  
 $\Theta_s$  is saturated water content.

#### References

1. Kozeny, J. Grund was serbewegungbeifreiem Spiegel, Fluss und Kanalversickerung. *Wasserkraft und Wasserwirtschaft*, 26, p. 3, 1931.
2. Vedernikov, V. Versickerungenaus Kanalen. *Wasserkraft und Wasserwirtschaft*, 11-13, p. 82, 1934.
3. Dachler, R., *Grundwasserstromung*. Springer, Wien, 1936.
4. Bouwer, H. "Theoretical Aspects Of Seepage From Open Channels", *Journal Of Hydraulics Division*, 91, pp. 37-59, 1965.
5. Bouwer, H. "Theory Of Seepage From Open Channels. In: V.T. Chow", *Advances In Hydroscience*, 5, Academic Press, New York., pp. 121-172, 1969.
6. Swamee P. K., Mishra G. C., and Chahar B. R., "Design of Minimum Seepage Loss Canal Sections", *Journal of Irrigation and Drainage Engineering*, 126 (1) pp. 28-32, 2000.
7. Uchdadiya, K. D., Patel. J. N., "Seepage Losses Through Unlined And Lined Canals", *International Journal of Advances in Applied Mathematics and Mechanics* 2(2) pp. 88 – 91, 2014.
8. Skaggs, T.H., Trout, T.J., Simunek, J., Shouse, P.J. "Comparison Of HYDRUS-2D Simulations Of Drip Irrigation With Experimental Observations", *Journal of Irrigation and Drainage Engineering ASCE* 130 Vol.4, pp. 304–310, 2004.
9. Siyal A.A., Skaggs T.H. "Measured And Simulated Soil Wetting Patterns Under Porous Clay Pipe Sub-Surface Irrigation" *Agricultural Water Management* Vol. 96, pp. 893–904, 2009.
10. Van Genuchten, M. Th. "A Closed-Form Equation For Predicting The Hydraulic Conductivity Of Unsaturated Soils" *Soil Science Soc. Am. J. Vol. 44*, pp. 892–898, 1980.
11. Mualem, Y. "A New Model For Predicting The Hydraulic Conductivity Of Unsaturated Porous Media" *Water Resource Research* Vol. 12, pp. 513–522, 1976.
12. Schaap, M. G., Leij, F. J., and van Genuchten, M. Th., "Rosetta: A Computer Program For Estimating Soil Hydraulic Parameters With

- Hierarchical Pedotransfer Functions”, *Journal of Hydrology*, 251, pp. 163-176, 2001.
13. Haykin, S. “Neural Networks: A Comprehensive Foundation”. McMillan, New York, 1994.
  14. Hassan A.E. and Hamed K.H., “Prediction Of Plume Migration In Heterogeneous Media Using Artificial Neural Networks”, *Water Resources Research*, 37(3), pp. 605–623, 2001.
  15. Fausett L.V., “Fundamentals Of Neural Networks: Architectures, Algorithms, And Applications”, Englewood Cliffs, NJ, Prentice-Hall, xvi, 461, 1994.
  16. Simunek, J., Sejna, M., van Genuchten, M. T. “The Hydrus Software Package For Simulating Two- And Three-Dimensional Movement Of Water, Heat, And Multiple Solutes In Variably-Saturated Media”, Technical Manual, Version 1.0, PC Progress, Prague, Czech Republic, pp. 241, 2006.
  17. Carsel, R.F., and Parrish, R.S. “Developing Joint Probability Distributions Of Soil Water Retention Characteristics”, *Water Resources Research* Vol. 24, pp. 755-769, 1988.

3/16/2019